
Energy-Based Transfer for Reinforcement Learning

Zeyun Deng[♣] Jasorsi Ghosh[♣] Fiona Xie[♣]
 Yuzhe Lu[◇] Katia Sycara[♣] Joseph Campbell[♣]
[♣] Purdue University [◇] AWS AI [♣] Carnegie Mellon University

Abstract

Reinforcement learning algorithms often suffer from poor sample efficiency, making them challenging to apply in multi-task or continual learning settings. Efficiency can be improved by transferring knowledge from a previously trained teacher policy to guide exploration in new but related tasks. However, if the new task sufficiently differs from the teacher’s training task, the transferred guidance may be sub-optimal and bias exploration toward low-reward behaviors. We propose an energy-based transfer learning method that uses out-of-distribution detection to selectively issue guidance, enabling the teacher to intervene only in states within its training distribution. We theoretically show that energy scores reflect the teacher’s state-visitation density and empirically demonstrate improved sample efficiency and performance across both single-task and multi-task settings.

1 Introduction

Reinforcement learning (RL) is a powerful tool for sequential decision-making [26; 15; 2], but credit assignment, sparse rewards, and modeling errors makes it notoriously sample inefficient. This is limiting in multi-task or continual learning settings, where agents must repeatedly learn to solve new tasks – particularly when those tasks are related to ones they have seen before. A natural question arises: *can we transfer knowledge from previously solved tasks to accelerate learning in new ones?*

One common approach to transfer is to reuse a previously trained teacher policy to guide a student policy’s exploration in a new task, either directly (by suggesting actions [5; 29; 18; 8; 9]) or indirectly (by shaping rewards [4; 11]). This form of transfer learning can be highly effective: early in learning, even partial guidance can steer the student toward high-reward behaviors and minimize the need for random exploration. However, when tasks are sufficiently different this approach can impair the student’s ability to learn; the teacher may issue sub-optimal guidance that biases exploration towards low-reward regions of the state-action space [27].

In this paper, we introduce an introspective transfer learning method that selectively guides exploration only when the teacher’s knowledge is likely to be helpful. Our approach, *energy-based transfer learning* (EBTL), is based on the insight that guidance should only be issued when the student visits states that lie within the teacher’s training distribution. Leveraging concepts from energy-based learning [14; 10] and out-of-distribution detection [16; 31; 23; 17], the teacher computes energy scores over states visited by the student during training, treating high-energy states as in-distribution and therefore eligible for guidance. This mechanism enables the teacher to act only when it is sufficiently “familiar” with the current context, leading to more efficient training – not by issuing *more* guidance but by issuing *correct* guidance.

Our contributions are as follows:

- We introduce an energy-based transfer learning method that selectively guides exploration only when the student’s state lies within the teacher’s training distribution.

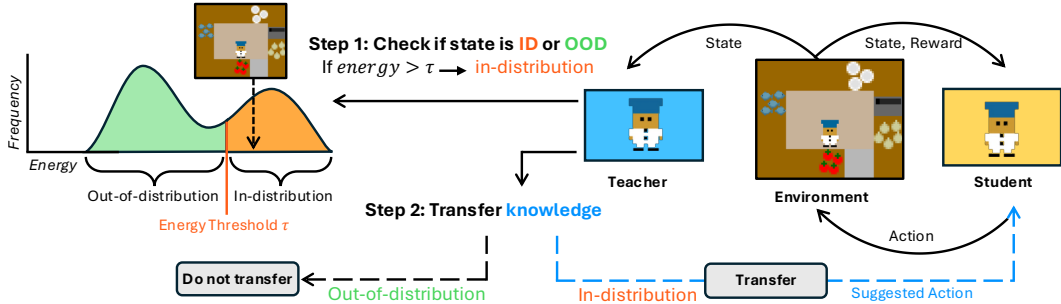


Figure 1: Overview of **energy-based transfer learning**. As the student interacts with the environment, the teacher: 1) checks if each state is in-distribution or out-of-distribution by comparing the state’s energy score to a pre-defined *energy threshold*; 2) If the state is greater than the *energy threshold*, then it is considered in-distribution for the teacher and an expert action is suggested to the student.

- We provide theoretical justification for our approach, showing that the energy score is proportional to the state visitation density induced by the teacher policy.
- We empirically demonstrate that our method yields more sample efficient learning and higher returns than standard reinforcement learning and transfer learning baselines, across both single-task and multi-task settings.

2 Related Work

Reinforcement learning provides a general framework for sequential decision-making, where an agent interacts with an environment to learn a policy that maximizes expected long-term reward [26]. However, RL methods typically require large amounts of experience, making them sample-inefficient – especially in sparse-reward or high-dimensional environments [1; 22].

To improve sample efficiency, transfer learning reuses knowledge acquired from prior tasks to accelerate learning in new ones [30]. In RL, this is commonly realized through a teacher-student paradigm, where a teacher policy trained on a source task provides guidance to a student learning a related target task [27; 33]. This guidance can take various forms, including action suggestions [28], reward shaping [19], and policy initialization [13]. Among these, parameter-based methods such as fine-tuning are the simplest, directly initializing the student’s parameters from the pretrained teacher policy and then adapting them through further training on the target task [32; 21]. However, parameter initialization alone can overly bias the student toward exploiting teacher behaviors, limiting exploration and resulting in suboptimal performance when the tasks differ.

Alternatively, behavior-based transfer methods explicitly encourage the student to mimic the teacher’s policy during training. One widely-used approach is *policy distillation*, where an auxiliary loss term encourages the student to replicate the teacher’s actions by minimizing divergence between the policies [24; 25]. In contrast, in *action advising* the teacher actively guides the student’s exploration by suggesting actions during training. A key challenge is determining when guidance should be issued, as early work showed that poorly timed advice can hinder learning [28]. To mitigate this, recent work has explored dynamic advising strategies. *JumpStart RL* [29] restricts guidance to a pre-defined episode prefix (i.e. the first h steps of an episode), while *introspective action advising* [5] uses deviations in the teacher’s expected reward to decide when to intervene.

However, prior methods rely on pre-defined heuristics, hyperparameters, or brittle fine-tuning strategies which limit their generalizability. Our method addresses this gap by applying theoretically-grounded out-of-distribution detection to reliably estimate teacher familiarity with a given state, enabling positive transfer performance even between tasks with high degrees of covariate shift.

3 Background

Reinforcement Learning. We model our setting as a Markov Decision Process (MDP), defined by the tuple $(\mathcal{S}, \mathcal{A}, P, R, \gamma)$, where \mathcal{S} is the set of states, \mathcal{A} is the set of actions, $P(s' | s, a)$ denotes

the transition probability from state s to state s' given action a , $R(s, a)$ is the reward function, and $\gamma \in [0, 1)$ is the discount factor. At each timestep t , the agent observes a state $s_t \in \mathcal{S}$, selects an action $a_t \in \mathcal{A}$, transitions to a new state $s_{t+1} \sim P(\cdot | s_t, a_t)$, and receives a reward $r_t = R(s_t, a_t)$. We consider the infinite-horizon setting, where our objective is to learn a policy $\pi(a | s)$ that maximizes the expected discounted return: $\mathbb{E}_\pi [\sum_{t=0}^{\infty} \gamma^t r_t]$.

Energy-Based Out-of-Distribution Detection. In this paper, we are interested in determining whether a state lies within the training distribution of a given policy. In supervised learning, this is broadly referred to as out-of-distribution (OOD) detection. A widely-used baseline for OOD detection uses the maximum softmax probability assigned to a predicted label [12]. However, softmax scores are not always reliable as neural networks can produce overconfident predictions for OOD states [20]. An alternative approach is to use the scalar *energy* of a state, which is computed from the raw logits of a network and has been shown to better separate in- and out-of-distribution examples [16].

Formally, given an input $\mathbf{x} \in \mathbb{R}^D$ and a neural network $f(\mathbf{x}) \in \mathbb{R}^K$ with logits $f_1(\mathbf{x}), \dots, f_K(\mathbf{x})$, we define the *free energy* for \mathbf{x} as follows, where $T > 0$ is a temperature parameter controlling the sharpness of the scaled logits:

$$E(\mathbf{x}; f) = -T \log \sum_{i=1}^K e^{f_i(\mathbf{x})/T}. \quad (1)$$

An input is considered to be OOD if $E(\mathbf{x}; f) > \tau$ for an *energy threshold* τ and in-distribution (ID) otherwise. The energy threshold is pre-computed over a set of in-distribution data.

4 Energy-Based Transfer Learning

Our goal is to improve the sample efficiency of reinforcement learning, which is particularly important in multi-task settings where the agent must learn to solve many (potentially related) tasks. One way to improve sample efficiency is to leverage a teacher policy trained on a related source task to guide the student in a new target task. However, naively applying teacher guidance can degrade sample efficiency if the student visits states outside the teacher’s training distribution, potentially biasing exploration toward uninformative or low-reward regions of the state-action space.

To address this, we propose a transfer learning framework in which the teacher suggests actions to the student only in states sufficiently close to the teacher’s training distribution. We formalize the problem of when to issue guidance as *out-of-distribution detection for reinforcement learning*.

Problem Formulation. Let π_T and π_S denote the teacher and student policies, respectively. We denote a trajectory as $X = \{x_t\}_{t=1}^n$, where each transition $x_t = (s_t, a_t, s_{t+1}, r_t)$ consists of the state s_t , action a_t , next state s_{t+1} , and reward r_t . We define a score function $\phi(s; \pi)$, where a state s is considered ID with respect to a policy π if $\phi(s) \geq \tau$, for some threshold $\tau \in \mathbb{R}$, and OOD otherwise. The action selection rule is then defined as:

$$a = \begin{cases} a_T \sim \pi_T(\cdot | s), & \text{if } \phi(s; \pi_T) \geq \tau, \\ a_S \sim \pi_S(\cdot | s), & \text{if } \phi(s; \pi_T) < \tau. \end{cases} \quad (2)$$

Equation 2 restricts teacher intervention to states sufficiently close to those it has seen during training, deferring to the student policy in all other cases.

4.1 Energy Scores and State Visitation

We draw inspiration from recent work on energy-based out-of-distribution detection [16] and define our score function as the negative free energy of a state s under the teacher policy:

$$\phi(s; \pi_T) = -E(s; \pi_T),$$

where $E(s; \pi_T)$ is the free energy computed from the teacher’s network. We refer to $\phi(s; \pi_T)$ as the energy score, which serves as a proxy for how likely the state is to belong to the teacher’s training distribution $p(x)$. In on-policy reinforcement learning, training data is generated by rolling out the teacher policy π_T to collect experience. As a result, $p(x)$ is implicitly defined by the state-visitation distribution $d_\pi(s)$ of the teacher. Consequently, the free energy $E(s; \pi_T)$ is negatively related with

the teacher’s familiarity with a state – assigning lower values to frequently visited states and higher values to unfamiliar ones. Following convention [16], we set the energy score ϕ to the *negative* free energy so that in-distribution states yield higher scores than out-of-distribution states.

Proposition 4.1. *Under on-policy training, let $d_\pi(s)$ denote the state-visitation distribution induced by policy π . Then the log of the visitation density is proportional to the score function $\phi(s) = -E(s)$:*

$$\log d_\pi(s) \propto \phi(s).$$

Proof. Given an energy-based model f , the density $p(s)$ is defined in terms of its energy $E(s)$ [14]:

$$p(s; f) = \frac{e^{-E(s; f)/T}}{Z}, \text{ where } Z = \int_s e^{-E(s; f)/T} \text{ is the partition function and } T \text{ is the temperature.}$$

Ignoring the normalizing constant Z and taking the logarithm of both sides we obtain:

$$\log p(s) \propto -E(s).$$

In on-policy RL, training data is collected by sampling trajectories under the current policy π . Thus, the empirical distribution $p(s)$ corresponds to the marginal distribution over states visited by π – the state-visitation distribution $d_\pi(s)$. Substituting this into the equation above, we obtain:

$$\log d_\pi(s) \propto -E(s) = \phi(s).$$

□

Algorithm 1 Energy-Based Transfer for Reinforcement Learning

Input: Teacher policy π_T , student policy π_S , energy threshold τ , decay function δ
while not done **do**
 Initialize empty batch $B \leftarrow \emptyset$
 for $t = 1 \rightarrow H$ **do**
 Sample $p \sim \mathcal{U}(0, 1)$ ▷ Sample probability of issuing guidance
 $a_t \leftarrow \begin{cases} \pi_T(a | s_t) & \text{if } -E(s_t; \pi_T) \geq \tau \text{ and } p < \delta(t) \\ \pi_S(a | s_t) & \text{if } -E(s_t; \pi_T) < \tau \end{cases}$ ▷ If s_t is in-distribution
▷ If s_t is out-of-distribution
 Take action a_t , observe r_t, s_{t+1}
 $B \leftarrow B \cup (s_t, a_t, s_{t+1}, r_t)$
 end for
 Update π_S with batch B ▷ Any on-policy update
end while

4.2 Algorithm

We summarize our approach in Algorithm 1. At a high-level, the student policy interacts with the environment to collect trajectories, while selectively receiving guidance from a teacher policy. At each timestep, EBTL evaluates whether the current state is familiar to the teacher using an energy-based OOD score. If the state is deemed in-distribution and a decaying probability schedule permits guidance, the action is sampled from the teacher policy; otherwise, the student policy acts. The resulting trajectories are stored in a batch and used to update the student policy. To decide when to issue guidance, we compute τ (see Equation 2) as the empirical q -quantile of energy scores over teacher training states \mathcal{S}_T , i.e., $\tau = \text{Quantile}_q(\{\phi(s) | s \in \mathcal{S}_T\})$. Following prior work [25; 29; 5], we apply a linear decay schedule $\delta(t) = \max(0, \delta_0 - \kappa t)$ to control the probability of guidance. This enables early reliance on the teacher while gradually promoting student autonomy.

Energy Regularization. As discussed in Section 4.1, the score function $\phi(s)$ is related to the teacher’s state-visitation frequency: frequently visited states tend to receive higher scores. However, this implicit signal may be insufficient to reliably distinguish ID from OOD states, as the teacher is trained solely on trajectories from its own environment and lacks exposure to OOD samples.

To improve separability, we adopt the energy-based loss from Liu et al. [16], augmenting the teacher’s training with a fixed set of representative OOD states. Let $\mathcal{D}_{\text{in}}^{\text{train}}$ denote the set of ID states collected

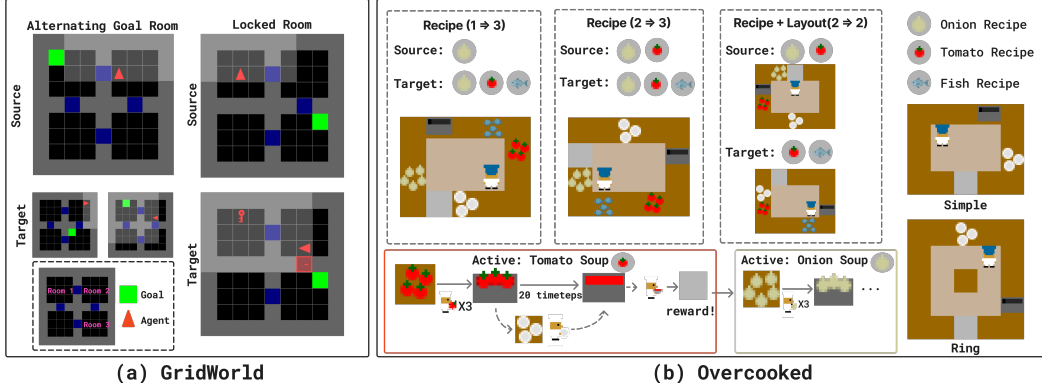


Figure 2: Environments used for empirical experiments. Refer to Section 5 for detailed descriptions.

during teacher training and $\mathcal{D}_{\text{out}}^{\text{train}}$ a curated set of OOD states. Let $\mathbf{s}_{\text{in}} \sim \mathcal{D}_{\text{in}}^{\text{train}}$ and $\mathbf{s}_{\text{out}} \sim \mathcal{D}_{\text{out}}^{\text{train}}$ denote samples from each. Using the energy score $\phi(s) = -E(s)$, the loss is defined as:

$$\mathcal{L}_{\text{energy}} = \mathbb{E}_{\mathbf{s}_{\text{in}}} \left[(\max(0, m_{\text{in}} - \phi(\mathbf{s}_{\text{in}}))^2 \right] + \mathbb{E}_{\mathbf{s}_{\text{out}}} \left[(\max(0, \phi(\mathbf{s}_{\text{out}}) - m_{\text{out}}))^2 \right],$$

where $m_{\text{in}} \in \mathbb{R}$ and $m_{\text{out}} \in \mathbb{R}$ are margin thresholds for ID and OOD energy scores, respectively. The first term penalizes ID states with energy scores below m_{in} ; the second penalizes OOD states with energy scores above m_{out} . The overall teacher loss is $\mathcal{L}_{\text{total}} = \mathcal{L}_{\text{RL}} + \lambda \cdot \mathcal{L}_{\text{energy}}$ where $\lambda \in \mathbb{R}^+$ controls the weight of the energy regularization. In EBTL, OOD samples are drawn from random policy rollouts in the target environment. ID samples are drawn from the teacher’s own training experience via random subsampling.

Off-Policy Correction. Actions sampled from the teacher policy, i.e. $a_t \sim \pi_T(\cdot | s_t)$, are inherently off-policy with respect to the student, and subsequently on-policy RL algorithms require a correction. In this work, we use proximal policy optimization (PPO) for training, and augment the actor and critic losses with an importance sampling ratio r_t . Let $\alpha_t \in \{0, 1\}$ denote whether the action at time t is sampled from the teacher policy ($\alpha_t = 1$) or the student policy ($\alpha_t = 0$). The clipped objective loss for the actor is given by:

$$\mathcal{L}^{\pi} = \hat{\mathbb{E}}_t \left[\min(r_t \hat{A}_t, \text{clip}(r_t, 1 - \epsilon, 1 + \epsilon) \hat{A}_t) \right], \quad r_t = \begin{cases} \frac{\pi_{\theta_S}(a_t | s_t)}{\pi_{\theta_{\text{old}}}(a_t | s_t)} & \text{if } \alpha_t = 0, \\ \frac{\pi_{\theta_S}(a_t | s_t)}{\pi_{\theta_T}(a_t | s_t)} & \text{if } \alpha_t = 1. \end{cases} \quad (3)$$

Here, θ_S denote the current parameters of the student policy π_S ; θ_{old} denotes the behavior policy used by π_S at data collection time; and θ_T denotes the frozen parameters of the teacher policy π_T . The estimated advantage at timestep t is denoted $\hat{A}_t \in \mathbb{R}$, and $\epsilon \in \mathbb{R}^+$ is the clipping threshold. The value function $V : \mathcal{S} \rightarrow \mathbb{R}$ estimates the expected return from state s_t , and is trained with the same importance ratio: $\mathcal{L}^V = \hat{\mathbb{E}}_t [r_t (V(s_t) - V_t^{\text{target}})^2]$, where V_t^{target} is the bootstrapped target and γ is the discount factor. Equation (3) ensures valid updates under mixed-policy rollouts.

5 Experiments

We evaluate our method in two settings: **single-task transfer** and **multi-task transfer**. The single-task setting is a Minigrad-based [7] environment composed of navigation tasks, where the agent’s objective is simply to reach a goal location. In the multi-task setting, we use Overcooked [6], where the agent must learn to solve multiple task variants, such as how to cook different recipes. For each setting, we construct multiple experimental scenarios that introduce increasing covariate shift between the teacher’s training distribution and the student’s target distribution. This allows us to evaluate the robustness of our method under progressively harder transfer scenarios.

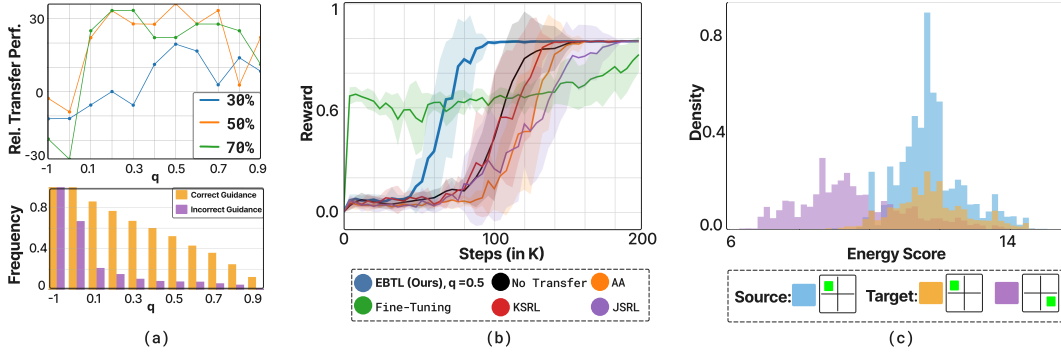


Figure 3: **Alternating-Goal** results. Results are averaged across 10 seeds. **(a, Top)** Relative transfer performance (in %) for varying energy thresholds and decay schedules (50% means the guidance probability decays to 0 when training is 50% done). A threshold of -1 indicates that guidance is given in all states. **(a, Bottom)** The rate at which correct and incorrect guidance is issued for each threshold; guidance is considered correct if it is issued for in-distribution states. **(b)** Evaluation returns for EBTL and baselines. **(c)** Empirical energy score distributions with respect to the teacher policy. The source task (blue) shows the teacher’s training distribution. The target task (orange + purple), measured during transfer, is bimodal: one mode overlaps with the source (shared sub-task, in-distribution), while the other does not (non-shared sub-task, out-of-distribution).

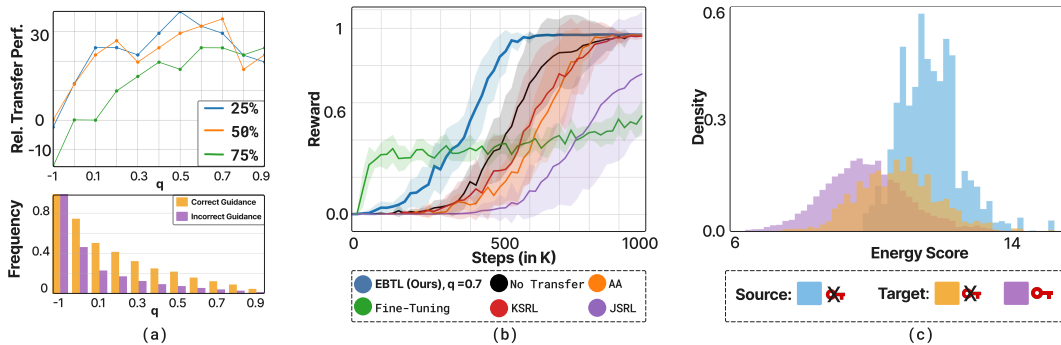


Figure 4: **Locked Room** results (10 seeds). See Figure 3 for caption details.

In each domain, we examine learning performance with the goal of understanding: (1) whether our method leads to improved sample efficiency, and (2) when the teacher chooses to provide guidance during the student’s learning process.

We compare our approach, energy-based transfer learning, against the following baselines:

- **No Transfer:** An agent trained from scratch with standard RL.
- **Action Advising (AA):** A teacher provides advice at every timestep. Advice issue rate decays over time using a predefined schedule.
- **Fine-Tuning:** The student is initialized from a pretrained teacher policy. Convolutional layers are frozen, and only the remaining parameters are updated during training.
- **Kickstarting RL (KSRL)** [25]: A policy distillation method that adds a decaying cross-entropy loss between the student and teacher policies to encourage imitation.
- **JumpStart RL (JSRL)** [29]: A time-based advising method where the teacher provides guidance only during the early part of each episode, with a decaying timestep threshold.

All experiments use teacher and student policies trained with the TorchRL [3] implementation of proximal policy optimization [25]. Full hyperparameter details are provided in the Appendix.

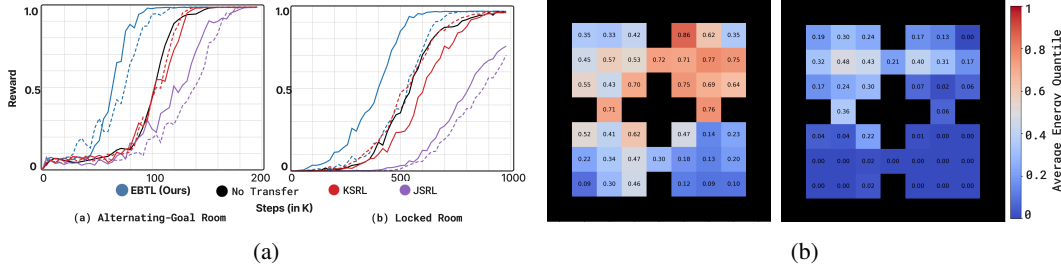


Figure 5: **(a)** Transfer performance with (solid) vs. without (dashed) energy regularization. **(b)** Heatmaps showing the average energy quantile of each state under the teacher policy for Alternating Goal Room. Left: source task where the goal is always in Room 1 (upper-left). Right: target task states collected only when the goal is placed in Room 3 (lower-right). Higher quantiles indicate greater teacher familiarity.

5.1 Single-Task Setting: Minigrid

Our Minigrid environment consists of four interconnected rooms and serves as a controlled single-task setting. We design two transfer setups, as illustrated in Figure 2a:

(1) Alternating Goal Room. The source task always places the goal in a random location in Room 1 (upper-left), while the target task randomly places it in either Room 1 (upper-left) or Room 3 (lower-right). The teacher should intervene only when the goal is in Room 1, where its prior experience applies; when the goal is in Room 3, the student must act independently.

(2) Locked Room. The source task allows free movement between rooms, while the target task introduces a locked door between the upper and lower areas. To reach the goal, the agent must first retrieve a key – randomly placed in the upper rooms – and unlock the door. Since the teacher was not trained to find or use a key, it should only provide guidance after the key has been picked up, when the remaining navigation matches its prior experience.

The results for the Alternating Goal Room and Locked Room setups are illustrated in Figure 3 and Figure 4, respectively. We make the following observations.

EBTL consistently outperforms all baselines. In both transfer setups, EBTL achieves the highest sample-efficiency of all baselines. For Alternating Goal Room, when the energy threshold $q \geq 0.1$, and for Locked Room, when $q > 0.1$, EBTL rarely issues guidance in unfamiliar states, leading to significant improvements in transfer performance. As shown in Figure 5b, the teacher correctly assigns higher energy scores to states encountered during training – when the goal is in Room 1 (upper-left) – compared to unseen states with the goal in Room 3 (lower-right).

Higher covariate shift makes OOD detection more challenging. In Alternating Goal Room, the teacher is able to clearly separate ID from OOD states, as reflected by the well-separated energy distributions in Figure 3c. However, in Locked Room, the introduction of novel elements – such as the door and key – creates a stronger covariate shift, making it harder for the teacher to correctly estimate familiarity. As shown in Figure 4c, the separation between ID and OOD states becomes less distinct. Despite this, the teacher still assigns consistently lower energy scores to pre-key states compared to post-key states, indicating that it can still meaningfully differentiate between unfamiliar and familiar regions of the state space.

There exists an optimal energy threshold q that balances filtering harmful and helpful guidance. The performance curves exhibit a mountain-shaped trend: increasing q initially boosts transfer performance by suppressing harmful advice in unfamiliar states. However, when q becomes too large, the teacher begins to withhold guidance even in familiar situations, limiting its usefulness. This trade-off is evident in both Figure 3a and Figure 4a, where performance declines once $q > 0.7$ due to overly conservative advising.

Energy regularization significantly improves EBTL but has little effect on other methods. As shown in Figure 5a, incorporating energy loss enables EBTL to converge faster, especially in the more challenging Locked Room environment where covariate shift is greater. In contrast, other baselines show no noticeable difference in performance regardless of whether the teacher was trained with or

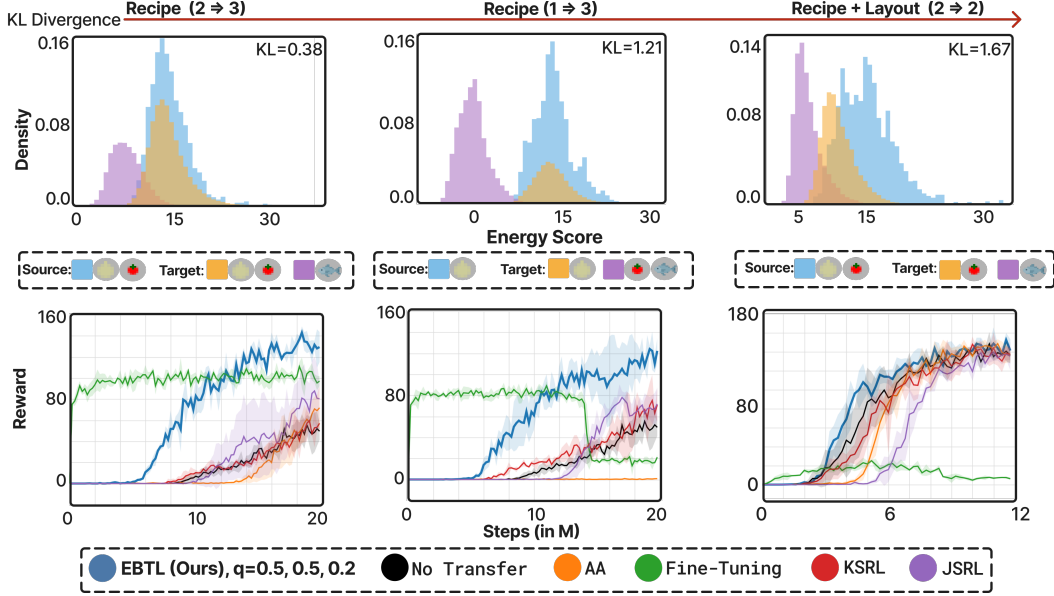


Figure 6: **Simple Room** results. Results are averaged across 3 seeds. **(Top)** Empirical energy score distributions with respect to the teacher policy. The source task (blue) shows the teacher’s training distribution. The target task (orange + purple), measured during transfer, is bimodal: one mode overlaps with the source (shared sub-task, in-distribution), while the other does not (non-shared sub-task, out-of-distribution). **(Bottom)** Evaluation returns for EBTL and baselines. Quantiles are set to $q = 0.5$ for Recipe Shift and $q = 0.2$ for the Recipe + Layout Shift.

without energy regularization – their convergence times remain similar. Notably, even without energy loss, EBTL still matches or exceeds all baselines, highlighting the robustness of our approach.

5.2 Multi-Task Setting: Overcooked

We create a single-agent variant of the popular Overcooked [6] environment designed to evaluate long-horizon multi-task learning. At each timestep, exactly one recipe – onion, tomato, or fish soup – is active, and the agent must prepare it by placing three matching ingredients into a pot. Once the soup is cooked (after a 20-step wait), the agent must retrieve a dish and deliver the soup to the serving station to receive a reward. A new recipe is randomly selected from the allowed set after each delivery, regardless of correctness. Rewards are sparse and given only for correct deliveries, with additional shaping applied to accelerate training. An overview of the setup is shown in Figure 2b, although we note that the locations of the ingredients, pot, and serving station are randomized. We evaluate on two layouts of increasing complexity: a simple room and a ring-shaped room. For each layout, we construct three Overcooked transfer setups with increasing levels of covariate shift between the teacher and student environments:

1. **Recipe Shift (2 \Rightarrow 3):** Both the source and target environments include all three ingredients: onions, tomatoes, and fish. The source task requires onion and tomato soup, while the target task requires onion, tomato, and fish soup resulting in recipe shift.
2. **Recipe Shift (1 \Rightarrow 3):** Both environments again have all three ingredients. This time, the source task requires only onion soup while the target task requires onion, tomato, and fish soup, introducing a higher degree of recipe shift.
3. **Recipe + Layout Shift (2 \Rightarrow 2):** The source environment includes only onions and tomatoes and requires onion and tomato soup, while the target environment includes only tomatoes and fish and requires recipe and layout. This results in both recipe and layout shift.

The results for the Simple Room and Ring Room setups are shown in Figure 6 and Figure 7, respectively. The relative difficulty of each transfer scenario is reflected by the increasing KL divergence between the energy score distributions over source and target states.

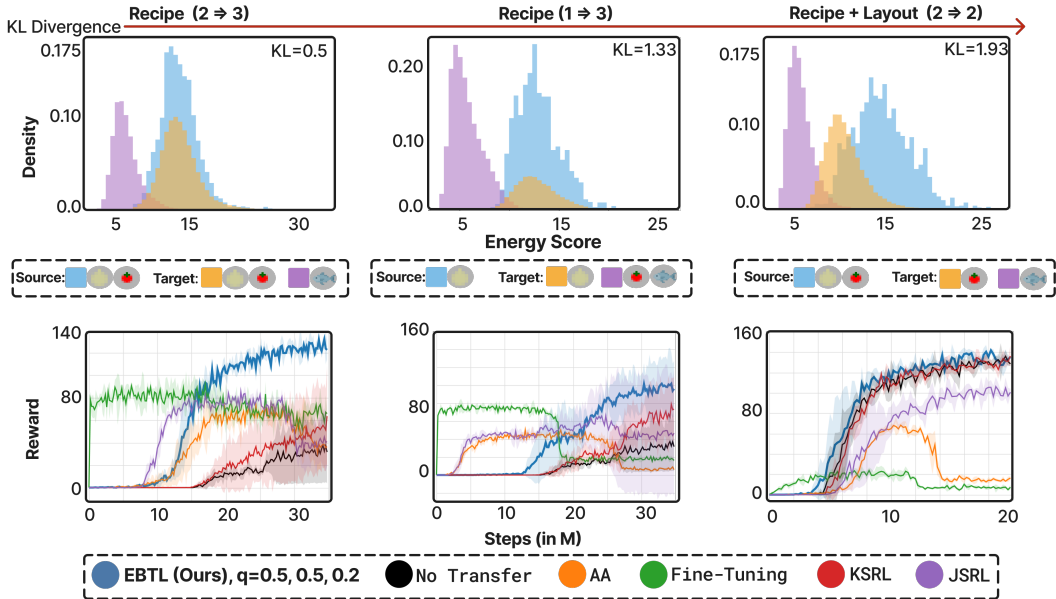


Figure 7: **Ring Room** results (3 seeds). See Figure 6 for caption details.

EBTL maintains positive transfer under increasing covariate shift. EBTL consistently outperforms all baseline methods in both sample efficiency and final policy return across all scenarios. As covariate shift between the source and target environments increases, transfer becomes more challenging. This is evident in the slower convergence from Recipe (2 \Rightarrow 3) to Recipe (1 \Rightarrow 3) in the Ring Room (Figure 7), where the teacher is only familiar with 1 rather than 2 recipes (out of 3 total). Despite this, EBTL yields positive transfer performance by restricting guidance to states associated with recipes that the teacher has encountered during training.

Shared layouts simplify OOD detection. In scenarios where the source and target tasks share spatial layouts, i.e. Recipe (2 \Rightarrow 3) and Recipe (1 \Rightarrow 3), the covariate shift is due entirely to the recipe encoding in the observation. This results in a clearly bimodal energy distribution in the target task – one mode for ID states and another for OOD – simplifying the OOD detection problem (refer to the top row of Figure 6 and Figure 7). However, when the layout changes, as in Recipe + Layout (2 \Rightarrow 2), there is a systematic decrease in ID energy scores, blurring the ID/OOD boundary. This is because even states associated with familiar recipes appear slightly OOD due to the layout shift.

Robustness to layout complexity. EBTL achieves stable positive transfer across both the Simple Room and Ring Room environments, resulting in high returns and low variance across seeds. In contrast, baseline methods without selective guidance, such as action advising (AA), see performance degradation as layout complexity increases. For example, in all three transfer settings in Figure 7, AA performance becomes unstable and reduces as training progresses, suggesting that an over-reliance on suboptimal advice increasingly impairs learning as the layout becomes more complex.

6 Conclusion and Limitations

We introduced energy-based transfer learning (EBTL), a method for improving sample efficiency in reinforcement learning by enabling selective teacher guidance. EBTL leverages energy scores as a proxy for familiarity, issuing advice only in states likely to lie within the teacher’s training distribution. Experiments across single-task and multi-task transfer settings demonstrate that EBTL consistently outperforms standard baselines, particularly under covariate shift.

Limitations. While effective, EBTL requires specifying an energy threshold and is primarily designed for settings with covariance rather than label shift. These limitations point to promising directions for future work on adaptive thresholding and broader forms of transfer.

References

- [1] Marcin Andrychowicz, Filip Wolski, Alex Ray, Jonas Schneider, Rachel Fong, Peter Welinder, Bob McGrew, Josh Tobin, OpenAI Pieter Abbeel, and Wojciech Zaremba. Hindsight experience replay. *Advances in neural information processing systems*, 30, 2017.
- [2] Kai Arulkumaran, Marc Peter Deisenroth, Miles Brundage, and Anil Anthony Bharath. Deep reinforcement learning: A brief survey. *IEEE Signal Processing Magazine*, 34(6):26–38, 2017.
- [3] Albert Bou, Matteo Bettini, Sebastian Dittert, Vikash Kumar, Shagun Sodhani, Xiaomeng Yang, Gianni De Fabritiis, and Vincent Moens. Torchrl: A data-driven decision-making library for pytorch, 2023.
- [4] Tim Brys, Anna Harutyunyan, Matthew E Taylor, and Ann Nowé. Policy transfer using reward shaping. In *AAMAS*, pages 181–188, 2015.
- [5] Joseph Campbell, Yue Guo, Fiona Xie, Simon Stepputtis, and Katia Sycara. Introspective action advising for interpretable transfer learning. In *Conference on Lifelong Learning Agents*, pages 1072–1090. PMLR, 2023.
- [6] Micah Carroll, Rohin Shah, Mark K Ho, Tom Griffiths, Sanjit Seshia, Pieter Abbeel, and Anca Dragan. On the utility of learning about humans for human-ai coordination. *Advances in neural information processing systems*, 32, 2019.
- [7] Maxime Chevalier-Boisvert, Bolun Dai, Mark Towers, Rodrigo Perez-Vicente, Lucas Willems, Salem Lahlou, Suman Pal, Pablo Samuel Castro, and Jordan Terry. Minigrad & mineworld: Modular & customizable reinforcement learning environments for goal-oriented tasks. In *Advances in Neural Information Processing Systems 36, New Orleans, LA, USA, December 2023*.
- [8] Yue Guo, Joseph Campbell, Simon Stepputtis, Ruiyu Li, Dana Hughes, Fei Fang, and Katia Sycara. Explainable action advising for multi-agent reinforcement learning. In *2023 IEEE International Conference on Robotics and Automation (ICRA)*, pages 5515–5521. IEEE, 2023.
- [9] Yue Guo, Xijia Zhang, Simon Stepputtis, Joseph Campbell, and Katia P. Sycara. Adaptive action advising with different rewards. In Vincenzo Lomonaco, Stefano Melacci, Tinne Tuytelaars, Sarath Chandar, and Razvan Pascanu, editors, *Proceedings of The 3rd Conference on Lifelong Learning Agents*, volume 274 of *Proceedings of Machine Learning Research*, pages 252–267. PMLR, 29 Jul–01 Aug 2025. URL <https://proceedings.mlr.press/v274/guo25a.html>.
- [10] Tuomas Haarnoja, Haoran Tang, Pieter Abbeel, and Sergey Levine. Reinforcement learning with deep energy-based policies. In *International conference on machine learning*, pages 1352–1361. PMLR, 2017.
- [11] Anna Harutyunyan, Sam Devlin, Peter Vrancx, and Ann Nowé. Expressing arbitrary reward functions as potential-based advice. In *Proceedings of the AAAI conference on artificial intelligence*, volume 29, 2015.
- [12] Dan Hendrycks and Kevin Gimpel. A baseline for detecting misclassified and out-of-distribution examples in neural networks. *arXiv preprint arXiv:1610.02136*, 2016.
- [13] Hao Ju, Rongshun Juan, Randy Gomez, Keisuke Nakamura, and Guangliang Li. Transferring policy of deep reinforcement learning from simulation to reality for robotics. *Nature Machine Intelligence*, 4(12):1077–1087, 2022.
- [14] Yann LeCun, Sumit Chopra, Raia Hadsell, M Ranzato, Fugie Huang, et al. A tutorial on energy-based learning. *Predicting structured data*, 1(0), 2006.
- [15] Yuxi Li. Deep reinforcement learning: An overview. *arXiv preprint arXiv:1701.07274*, 2017.
- [16] Weitang Liu, Xiaoyun Wang, John Owens, and Yixuan Li. Energy-based out-of-distribution detection. *Advances in neural information processing systems*, 33:21464–21475, 2020.

- [17] Yuzhe Lu, Yilong Qin, Runtian Zhai, Andrew Shen, Ketong Chen, Zhenlin Wang, Soheil Kolouri, Simon Stepputtis, Joseph Campbell, and Katia Sycara. Characterizing out-of-distribution error via optimal transport. *Advances in Neural Information Processing Systems*, 36:17602–17622, 2023.
- [18] Richard Maclin and Jude W Shavlik. *Incorporating advice into agents that learn from reinforcements*. University of Wisconsin-Madison. Computer Sciences Department, 1994.
- [19] Andrew Y Ng, Daishi Harada, and Stuart Russell. Policy invariance under reward transformations: Theory and application to reward shaping. In *Icml*, volume 99, pages 278–287. Citeseer, 1999.
- [20] Anh Nguyen, Jason Yosinski, and Jeff Clune. Deep neural networks are easily fooled: High confidence predictions for unrecognizable images. In *Proceedings of the IEEE conference on computer vision and pattern recognition*, pages 427–436, 2015.
- [21] Celal Öztürk, Murat Taşyürek, and Mehmet Uğur Türkdamar. Transfer learning and fine-tuned transfer learning methods’ effectiveness analyse in the cnn-based deep learning models. *Concurrency and computation: practice and experience*, 35(4):e7542, 2023.
- [22] Rémy Portelas, Cédric Colas, Lilian Weng, Katja Hofmann, and Pierre-Yves Oudeyer. Automatic curriculum learning for deep rl: A short survey. *arXiv preprint arXiv:2003.04664*, 2020.
- [23] Jie Ren, Peter J Liu, Emily Fertig, Jasper Snoek, Ryan Poplin, Mark Depristo, Joshua Dillon, and Balaji Lakshminarayanan. Likelihood ratios for out-of-distribution detection. *Advances in neural information processing systems*, 32, 2019.
- [24] Andrei A Rusu, Sergio Gomez Colmenarejo, Caglar Gulcehre, Guillaume Desjardins, James Kirkpatrick, Razvan Pascanu, Volodymyr Mnih, Koray Kavukcuoglu, and Raia Hadsell. Policy distillation. *arXiv preprint arXiv:1511.06295*, 2015.
- [25] Simon Schmitt, Jonathan J Hudson, Augustin Zidek, Simon Osindero, Carl Doersch, Wojciech M Czarnecki, Joel Z Leibo, Heinrich Kuttler, Andrew Zisserman, Karen Simonyan, et al. Kickstarting deep reinforcement learning. *arXiv preprint arXiv:1803.03835*, 2018.
- [26] Richard S Sutton, Andrew G Barto, et al. *Reinforcement learning: An introduction*, volume 1. MIT press Cambridge, 1998.
- [27] Matthew E Taylor and Peter Stone. Transfer learning for reinforcement learning domains: A survey. *Journal of Machine Learning Research*, 10(7), 2009.
- [28] Lisa Torrey and Matthew Taylor. Teaching on a budget: Agents advising agents in reinforcement learning. In *Proceedings of the 2013 international conference on Autonomous agents and multi-agent systems*, pages 1053–1060, 2013.
- [29] Ikechukwu Uchendu, Ted Xiao, Yao Lu, Banghua Zhu, Mengyuan Yan, Joséphine Simon, Matthew Bennice, Chuyuan Fu, Cong Ma, Jiantao Jiao, et al. Jump-start reinforcement learning. In *International Conference on Machine Learning*, pages 34556–34583. PMLR, 2023.
- [30] Karl Weiss, Taghi M Khoshgoftaar, and DingDing Wang. A survey of transfer learning. *Journal of Big data*, 3:1–40, 2016.
- [31] Jingkan Yang, Kaiyang Zhou, Yixuan Li, and Ziwei Liu. Generalized out-of-distribution detection: A survey. *International Journal of Computer Vision*, 132(12):5635–5662, 2024.
- [32] Jason Yosinski, Jeff Clune, Yoshua Bengio, and Hod Lipson. How transferable are features in deep neural networks? *Advances in neural information processing systems*, 27, 2014.
- [33] Zhuangdi Zhu, Kaixiang Lin, Anil K Jain, and Jiayu Zhou. Transfer learning in deep reinforcement learning: A survey. *IEEE Transactions on Pattern Analysis and Machine Intelligence*, 45(11):13344–13362, 2023.

Appendix

A Training Details

A.1 GridWorld

Reward Structure and Action Masking. In the MiniGrid experiments, agents are trained under a sparse reward setting: a reward of 1 is given only when the agent successfully reaches the goal location. No shaped or intermediate rewards are provided, making the task highly exploration-dependent. To mitigate the resulting challenge and accelerate learning, we apply action masking to dynamically restrict the agent’s action space based on its immediate environment. The action mask disables irrelevant or invalid actions at each timestep: (1) the *forward* action is masked out if the agent is facing a wall, preventing redundant collisions; (2) the *pickup* action is disabled unless the agent is directly facing a key; (3) the *toggle* action is masked out unless the agent is facing a door; (4) the *drop* action is always disabled, as object dropping is unnecessary in our tasks; and (5) the *done* action is permanently disabled, since it is not used in our environments. This selective pruning of the action space reduces the likelihood of unproductive behavior and enables the agent to focus on learning goal-directed policies more effectively.

Teacher Training. In both experimental setups, we train two variants of the teacher policy using standard Proximal Policy Optimization (PPO) in the source environment: one with the energy-based loss and one without. For the teacher trained with energy loss, the m_{in} and m_{out} are set to 10 and 15 respectively. These values are chosen arbitrarily, as the separation between energy distributions is insensitive to the exact threshold choice (see Section D). The training follows a consistent set of hyperparameters, as detailed in the next section. For the *unlocked-to-locked* environment, 800K-step checkpoints are selected from both training variants. For the *alternating-goal room* environment, 200K-step checkpoints are used.

Student Training. For each target task, we first train a student policy from scratch using standard PPO without any transfer to establish baseline performance. In the *unlocked-to-locked* environment, the total training horizon for transfer experiments is set to 1 million steps, while in the *alternating-goal room* environment, it is set to 200,000 steps. All experiments in the MiniGrid setups are conducted with 10 random seeds to ensure robustness. Within each domain, the student and teacher policies share the same model architecture.

A.2 Overcooked-AI

Reward Structure. In all Overcooked setups, no action masking is applied. Instead, shaped rewards are introduced to facilitate the training process. A shaped reward of 3 is given when the correct ingredient is added to a pot. An additional reward of 3 is awarded when a dish is picked up—provided there are no dishes already on the counter and the soup is either cooking or completed. A reward of 5 is granted when the soup is picked up. Furthermore, a shaped reward of 3 is given upon delivering the soup, regardless of whether it matches the currently active recipe. All shaped rewards follow a predefined linear decay schedule. In contrast, a sparse reward of 20 is awarded when the delivered soup matches the active recipe; this reward does not decay over time.

Teacher Training. In all Overcooked setups, teacher policies are trained in the source environment using standard Proximal Policy Optimization (PPO) with hyperparameters described in the following section. For each setup and source-target configuration, a specific checkpoint is selected to serve as the teacher for transfer. The table below lists the selected training step (in environment steps) corresponding to each teacher checkpoint.

Table 1: Selected teacher checkpoints (in environment steps) for each Overcooked setup and source-target configuration.

Setup	Recipe (2 → 3)	Recipe (1 → 3)	Recipe + Layout (2 → 2)
Simple Room	19,008,000	9,004,800	12,000,000
Ring Room	2,400,000	10,003,200	18,000,000

Student Training. In all Overcooked setups, student policies are trained in the target environment using PPO under a fixed transfer horizon. For the teacher trained with energy loss, the m_{in} and m_{out} are set to 12 and 14 respectively. The training is conducted using consistent hyperparameters, as detailed in the next section. All experiments are repeated with 3 random seeds to ensure stability and reproducibility. The transfer horizon varies depending on the setup and source-target configuration. The table below summarizes the number of environment steps used during student training for each case:

Table 2: Transfer horizons (in millions of environment steps) used for student training in each Overcooked setup and configuration. Each experiment is run with 3 random seeds.

Setup	Recipe (2 → 3)	Recipe (1 → 3)	Recipe + Layout (2 → 2)
Simple Room	20M	20M	12M
Ring Room	35M	35M	20M

B Hyperparameters

B.1 GridWorld

All experimental setups in GridWorld are trained using a fixed set of PPO hyperparameters, summarized in Table 3. These settings remain consistent across all teacher and student training runs within the domain.

Table 3: Hyperparameters used for all GridWorld experiments.

Hyperparameter	Value
Learning rate	0.0005
Discount factor (γ)	0.9
GAE lambda (λ)	0.8
Policy clip parameter	0.2
Value function clip parameter	10.0
Value loss coefficient	0.5
Entropy coefficient	0.01
Train batch size	256
SGD minibatch size	128
Number of SGD iterations	4
Number of parallel environments	8
Normalize advantage	False

B.2 Overcooked-AI

All Overcooked experiments use a shared set of core PPO hyperparameters, listed in Table 4. These settings are consistent across teacher and student training. However, the learning rate and reward shaping horizon vary depending on the layout and recipe configuration, summarized in Table 5. We use the following notation: O = Onion, T = Tomato, F = Fish, OT = Onion + Tomato, TF = Tomato + Fish, OTF = Onion + Tomato + Fish.

C Model Architecture

All MiniGrid experiments share the same model architecture shown in Fig. 8a. Similarly, all Overcooked experiments use the architecture in Fig. 8b. Due to layout size differences in Overcooked, the dense layer input size is set to 182 for *Simple* layouts and 257 for *Ring* layouts.

D Sensitivity of Energy-Based Separation

We evaluate whether varying the energy thresholds m_{in} and m_{out} affects the teacher’s ability to distinguish between false and true out-of-distribution (OOD) states. The energy loss used during

Table 4: Shared PPO hyperparameters across all Overcooked experiments.

Hyperparameter	Value
Discount factor (γ)	0.99
GAE lambda (λ)	0.6
KL coeff	0.0
Reward clipping	False
Clip parameter	0.2
VF clip parameter	10.0
VF loss coeff	0.5
Entropy coeff	0.1
Train batch size	9600
SGD minibatch size	1600
SGD iterations	8
Parallel envs	24
Normalize advantage	False

Table 5: Setup-specific learning rates and reward shaping horizons.

Layout	Config	LR	Horizon
Simple	Recipe (O)	0.001	8M
	Recipe (OT)	0.001	15M
	Recipe (OTF)	0.001	25M
	Recipe + Layout (OT)	0.001	10M
	Recipe + Layout(TF)	0.001	10M
Ring	Recipe (O)	0.0006	10M
	Recipe (OT)	0.0006	20M
	Recipe (OTF)	0.0006	30M
	Recipe + Layout (OT)	0.0006	15M
	Recipe + Layout (TF)	0.0006	15M

training is defined over the energy score $\phi(s) = -E(s)$ as:

$$\mathcal{L}_{\text{energy}} = \mathbb{E}_{\mathbf{s}_{\text{in}} \sim \mathcal{D}_{\text{in}}^{\text{train}}} \left[(\max(0, m_{\text{in}} - \phi(\mathbf{s}_{\text{in}})))^2 \right] + \mathbb{E}_{\mathbf{s}_{\text{out}} \sim \mathcal{D}_{\text{out}}^{\text{train}}} \left[(\max(0, \phi(\mathbf{s}_{\text{out}}) - m_{\text{out}}))^2 \right].$$

Experimental Setup Experiments are conducted in the *GridWorld (unlocked-to-locked)* environment. During training, the in-distribution (ID) set consists of the most recent 3,000 frames collected from the agent’s own trajectory. The out-of-distribution (OOD) set is fixed and sampled from 100 episodes of a random policy in the target environment, where the agent is randomly initialized in any room at the start of each episode to ensure unbiased state coverage (rather than being constrained to the upper room). We evaluate six combinations of $(m_{\text{in}}, m_{\text{out}})$ used in the energy regularization loss (defined over energy scores $\phi(s) = -E(s)$): (10, 15), (5, 10), (15, 20), (10, 10), (15, 15), (12, 14). Each configuration is trained with 3 random seeds using a shared PPO setup and evaluated at the 800,000-step checkpoint.

Sensitivity Evaluation Protocol. We assess whether the teacher consistently distinguishes between *false OOD* states – those similar to ID states and where guidance should be issued – and *true OOD* states – those clearly out-of-distribution and where guidance should be withheld. Both sets are drawn from a fixed OOD dataset collected via a random policy in the target environment. For each $(m_{\text{in}}, m_{\text{out}})$ configuration, we compute the divergence between the energy score distributions of false and true OOD states across three training seeds using Jensen-Shannon divergence, total variation distance, Hellinger distance, and Kullback-Leibler (KL) divergence. To evaluate sensitivity, we apply one-way ANOVA and Kruskal-Wallis tests to determine whether this separation remains consistent across different regularization settings. A high p-value indicates that the teacher’s ability to determine when to issue guidance is robust to the choice of $(m_{\text{in}}, m_{\text{out}})$.

Metric	ANOVA p-value	Kruskal-Wallis p-value
Jensen-Shannon	0.1138	0.1592
Kullback-Leibler	0.2457	0.1799
Total Variation	0.1728	0.2322
Hellinger Distance	0.1247	0.1592

Table 6: Statistical test results (p-values) for divergence between False OOD and True OOD energy distributions across different $(m_{\text{in}}, m_{\text{out}})$ settings.

Results. As shown in Table 6, we observe no statistically significant variation in the separation between false and true OOD states across different $(m_{\text{in}}, m_{\text{out}})$ configurations. The ANOVA and

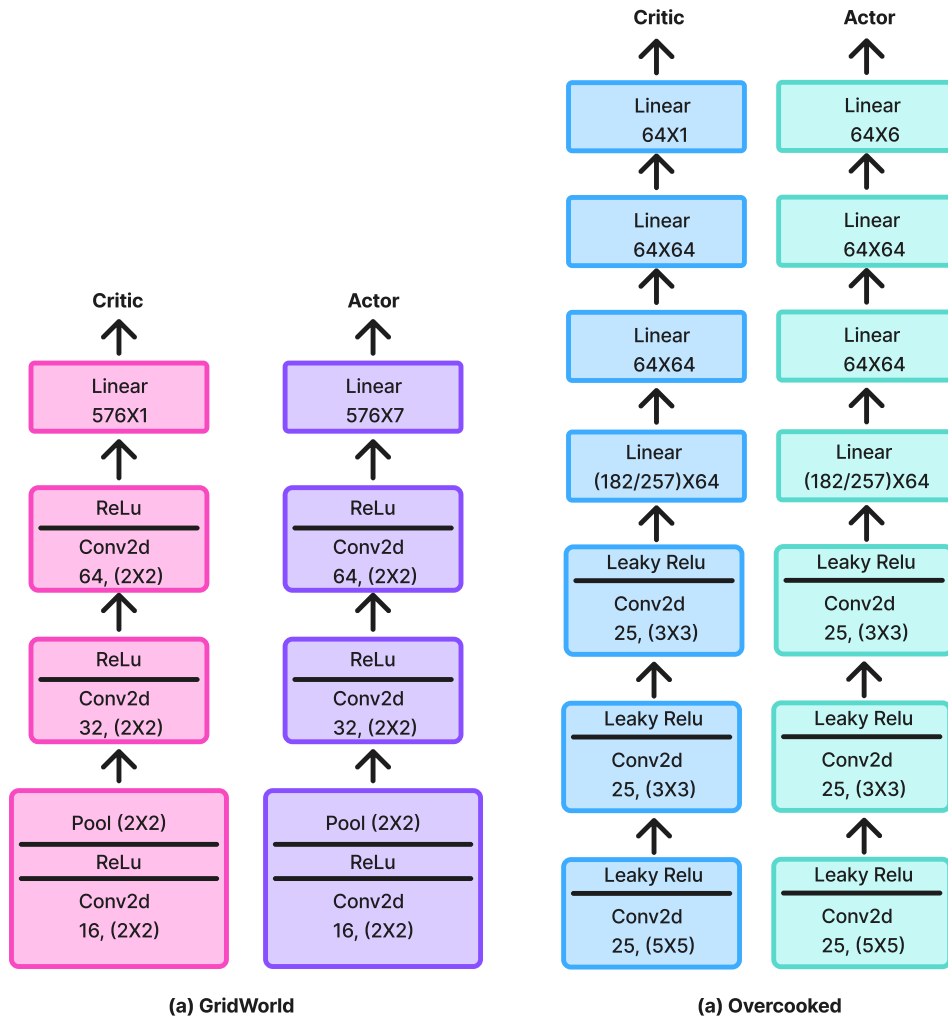


Figure 8: Actor-Critic architectures used in our experiments. (a) MiniGrid. (b) Overcooked.

Kruskal-Wallis tests yield p-values above 0.1 for all four divergence metrics, indicating that the teacher’s ability to distinguish between states where guidance should or should not be issued is stable across regularization settings.